Applications of FT Raman Spectroscopy and Micro Spectroscopy Characterizing Cellulose and Cellulosic Biomaterials

Steffen Fischer,[1] *Karla Schenzel,**[2] *Klaus Fischer,*[3] *Wulf Diepenbrock*[2]

[1] Fraunhofer Institute of Applied Polymer Research, Geiselbergstraße 69, 14476 Potsdam, Germany
E-mail: steffen.fischer@iap.fhg.de
[2] Agricultural Department, Martin Luther University Halle-Wittenberg,Ludwig-Wucherer-Str. 2, 06108 Halle, Germany
E-mail: schenzel@landw.uni-halle.de
[3] Institute of Plant and Wood Chemistry, Dresden University of Technology, Pienner Str. 19, 01737 Tharandt, Germany
E-mail: fischerk@forst.tu-dresden.de

Summary: FT Raman spectroscopy and micro spectroscopy were used for the investigation of cellulose, cellulose derivatives and cellulosic plant fibres. Lattice structures of cellulose, polymorphic modifications I and II, as well as amorphous structure, were clearly identified by means of FT Raman vibrational spectra. Chemometric models were developed utilizing univariate calibration as well as methods of multivariate data analyses of FT Raman spectral data for the fast prediction of cellulose properties. Cellulose properties like the degree of crystallinity Xc_{Raman}, the degree of substitution DS_{CMC}, DS_{AC} and cellulose reactivity were determined.
In situ/ in vivo FT Raman micro spectroscopy was used for the characterization of cellulose structures of flax and hemp fibres. Orientational and stress dependent FT Raman experiments were carried out.

Keywords: cellulose; cellulose derivatives; FT Raman spectroscopy; micro spectroscopy; plant fibres

Introduction

Vibrational spectroscopy, especially Raman spectroscopy, has played an important role in the investigation of cellulose structures. The fundamental studies of Atalla and co-workers confirmed the advantage of this analytical method over IR and NMR spectroscopy, for determining the molecular conformations and hydrogen bonding patterns of cellulose and cellulosic biomaterials.[1-9]

The main reason for the trend to Raman spectroscopy was the development of effective FT Raman spectrometers using NIR or red excitation lasers which avoid the fluorescence of

 DOI: 10.1002/masy.200550503

the samples which normally blank the Raman signals. The development of high sensitive detectors in conjunction with the coupling of optical fibres and microscopes enhanced the capacity of Raman spectroscopy for analytical analysis and online process control. FT Raman microscopes equipped with mapping units became very powerful tools especially for *in situ* investigations of biomaterials.[10-12]

We began a still ongoing examination of cellulose structures using methods of deconvolution of the FT Raman spectra, utilizing all the advantages of new spectrometers, computational technologies as well as methods for analysing the Raman vibrational spectra. We developed methods for quantification and fast prediction of cellulose properties using methods of spectra fine resolution in combination with multivariate analyses of the spectral data. Furthermore, we characterized the molecular structures and composition of cellulosic plant fibres of flax and hemp by means of different FT Raman and micro Raman experiments.

In this paper we report on new results and give a summary of past results of our FT Raman spectroscopic investigations on cellulose and cellulosic biomaterials, which clearly demonstrate the capability and convenience of this analytical method.

Investigations on Cellulose Structures

Cellulose Modifications I and II

FT Raman spectra of the polymorphic modifications cellulose I and II reflect the conformational differences of both lattice types most clearly in the low frequency range of the spectra, see Figure 1 (left). Obviously, cellulose modification I and II differ in the conformational arrangements of the side chains of the anhydroglucopyranose residues. Our findings by FT Raman experiments which were reported earlier[13], confirmed findings by Wiley & Atalla[5, 6] using "classical" Raman spectroscopy with visible laser excitation. The FT Raman spectra of cellulose modification I indicated the simultaneous presence of two stereo chemically non-equivalent CH_2OH groups resulting from the rotation of the side chains about the C(5)–C(6) atoms. In cellulose II, only one type of the CH_2OH groups was present. This causes the two scissoring vibrations of the methylene groups to merge into one single signal.

In contrast to the investigations of Atalla & co-workers, we recorded the Raman vibrational spectra by means of NIR laser excitation. Thus, fluorescence-free Raman spectra of cellulose, pulps and plant material were measured without special sample preparations. Furthermore, using methods of derivative spectrometry already small differences in the vibrational behaviour of cellulose modifications or cellulose forms were identified at their FT Raman spectra. For instance, the alkaline treatments of cellulose indicated a frequency shift $\Delta\nu$ of 13 cm^{-1} of the most intensive Raman line (2893 cm^{-1}), as can be seen from the second derivatives, see Figure 1 (right). After the treatments (c_{NaOH}= 16%) the intensity maximum appeared at 2880 cm^{-1}, which is a characteristic of cellulose modification II.[14]

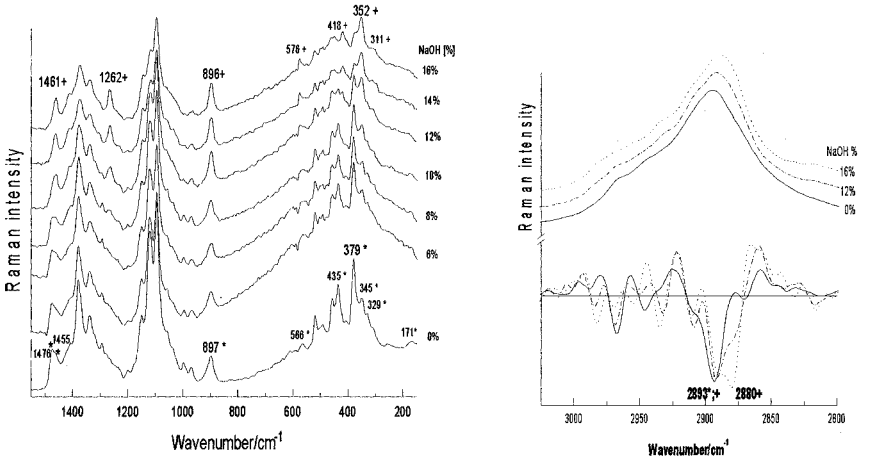

(*) cellulose modification I; (+) cellulose modification II

Figure 1. FT Raman spectra following the polymorphic transformation cellulose I into cellulose II due to cellulose treatments with different alkaline concentrations; (left): low frequency range; (right): CH stretching region of the spectra and their second derivatives.

The polymorphic transformation of cellulose I into cellulose II is caused also by dissolving cellulose in different molten inorganic salt hydrates. Previously, it was reported that several molten inorganic salt hydrates may serve as solvents for cellulose.[15-17] Interestingly, from cellulose, regenerated from the melts of $ZnCl_2 \cdot 4H_2O$, $LiSCN \cdot 2{,}5H_2O$ and $LiCl \cdot 2ZnCl_2 \cdot 6H_2O$, it can be proven that dissolution leads to the transformation of cellulose I to cellulose II. This was confirmed by FT Raman spectra and WAXS investigations.[13]

Amorphous Cellulose

The three molten salts $ZnCl_2+4H_2O$, $LiSCN•2,5H_2O$ and $LiCl+2ZnCl_2+6H_2O$ served as solvents for the cellulose for the dissolution experiments. Solutions of cellulose (5 % w/w) were prepared using the melt. Whereas solutions of cellulose in $ZnCl_2+4H_2O$ appeared liquid after rapid cooling to room temperature, solutions in $LiSCN•2,5H_2O$ and $LiCl+2ZnCl_2+6H_2O$ formed a glassy state. In all cases no precipitation of cellulose fibres was observed. It can be concluded, that the specific interactions between cellulose and molten salts within the solution are maintained also in the solid state after cooling.

The dissolving process could be controlled easily by online FT Raman spectroscopic investigations, because the pure molten salts do not show any vibrational mode at the observed frequency range of the FT Raman spectra. It turned out that the Raman lines of the dissolved cellulose are broader in the melt systems than for the pure polymers. Nevertheless, a Raman shift of the ν(C-O-C) modes of cellulose ($\Delta\nu$ of ~10 cm^{-1}) to lower wave numbers was observed indicating different vibrational coupling between the anhydroglucopyranose units when compared with the crystalline cellulose.

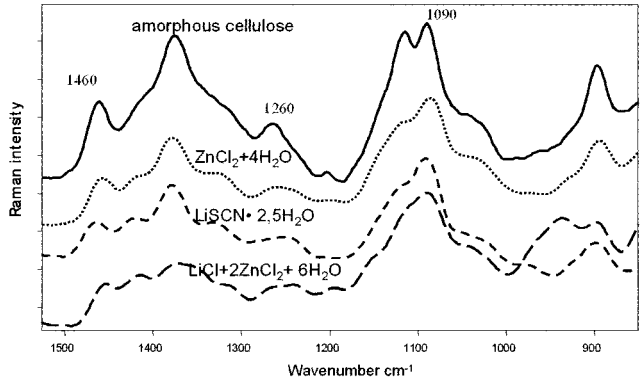

Figure 2. FT Raman spectra of amorphous cellulose in comparison to FT Raman spectra of cellulose dissolved in $ZnCl_2+4H_2O$, $LiSCN•2H_2O$ and $LiCl+2ZnCl_2+6H_2O$ recorded directly within the molten salts.

A comparison of the FT Raman spectra of amorphous cellulose with the spectra of cellulose dissolved in the hydrated melts is shown in Figure 2. It can easily be seen that the vibrational frequency of the ν(C-O-C) mode of cellulose in the melts and that of amorphous cellulose are nearly the same. Additionally, typical vibrations of amorphous

cellulose were observed at 1260 cm^{-1} and 1460 cm^{-1}. This was also the case for the cellulose in the hydrated melts. Therefore it was deduced, that cellulose dissolved in molten salts undergoes a transition into an amorphous state. This was also confirmed by ^{13}C NMR measurements.[16] No indication for the formation of additional compounds have been observed.

Crystalline and Amorphous Cellulose - Determination of Xc_{Raman}/%

In view of those results, it became interesting to examine the vibrational behaviour of crystalline cellulose I, and compare it with the amorphous forms, which were produced by grinding of the crystalline ones. Two model systems of cellulose I, a bacterial cellulose as well as an Eucalyptus sulphite pulp system were investigated. These also served as calibration models which represented entire ranges of cellulose I crystallinity of 0-69% and 0-40%.

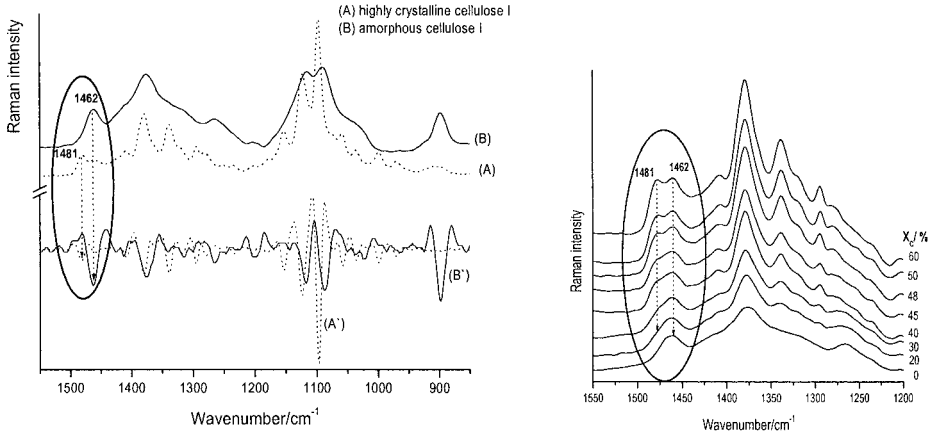

Figure 3. FT Raman spectra and second derivatives of cellulose I model compounds, (left). FT Raman spectra of generated mixtures of cellulose I with different adjusted degrees of crystallinity, Xc/ %, (right).

Once more, using methods of fine resolution of the convoluted FT Raman spectra of cellulose, significant differences between crystalline cellulose I and its amorphous form were observed in the range of δ CH_2 of the CH_2OH side chains of the cellulose skeletons. The vibrational modes of methylene bendings δ CH_2, characteristic of each

form, crystalline (1481 cm^{-1}) and amorphous (1462 cm^{-1}), were determined, see Figure 3 (left). A strong intensity dependence of these two peaks was observed due to the transition from crystalline to amorphous state, as it is presented in Figure 3 (right) by physical mixtures of cellulose I with different degrees of adjusted crystallinity, Xc/%: 0%; 10%; ...60%. As a result, the intensity ratio of the two characteristic lines is strongly influenced by the degree of crystallinity of cellulose I, and therefore also suitable for its quantification. Taking this into account, a Raman crystallinity index, Xc_{Raman} / % = (I_c / I_c +I_a) x 10^2, was defined to determine the percentage crystallinity -Xc_{Raman}- of cellulose I. Intensities of the Raman modes of crystalline (I_c) and amorphous (I_a) content were obtained by peak fitting using Gaussian bands and linear baselines. Linear calibration curves illustrating the relationship between experimentally determined percentage crystallinities, Xc_{Raman} and adjusted crystallinities, Xc, were obtained by least square analyses of the data for both model systems.

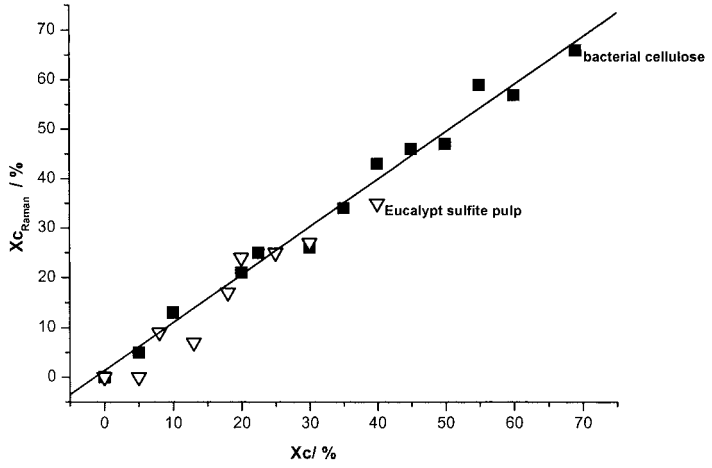

Figure 4. Eucalyptus sulphite pulp model (∇) included into the bacterial cellulose calibration set (■), described by Xc_{Raman} = 0.962 Xc + 1.34.

In Figure 4, the Eucalyptus sulphite pulp system was included into the bacterial cellulose calibration set. KBr was used for homogenisation of the powder blends to keep effects of light diffraction due to different refractive indices at a minimum. Thus, it became possible to describe the two cellulosic systems by one calibration model.

Microcrystalline cellulose with known Xc_{NMR} values were examined for validation of this univariate calibration model. Generally, Xc_{Raman} values and Xc_{NMR} values agree to within ± 5%. These investigations using methods of univariate spectra analysis led to the development of a new method for quantification of cellulose I crystallinity. This method is described in full somewhere else.[18]

Quantification and Prediction of Cellulose Properties

In accordance with the new spectroscopic approaches, it is necessary to establish reliable and rapid methods to perform FT Raman analyses for quantification or for prediction of physical and chemical properties also of such complex molecules like cellulose and high variable systems like biological materials. For these purposes, methods of multivariate calibration, classification and clustering of the analytical data may be used.

Determination of Xc_{Raman} - a Multivariate Calibration Model

The cellulose I model systems with known percentual crystallinity values Xc_{Raman}/% that were obtained by means of the univariate calibration model as described above were examined using the Bruker OPUS/Quant 2 software. A partial least square algorithm (PLS) was utilized in order to find the best correlation function between spectral and concentration matrix. A very fast multivariate chemometric calibration model for predicting the percentage of cellulose crystallinity, Xc_{Raman} /% was developed by applying cross-validation.[19] In Table 1 the Xc_{Raman}/ % values of different cellulose determined by means of the univariate as well as the multivariate calibration model are presented and compared with the corresponding Xc_{NMR} values.

It is necessary that the number of calibration spectra exceeds the number of components in the mixture in order to obtain statistically significant results for PLS software. 22 FT Raman spectra, one for each generated cellulose I mixture with known degree of crystallinity Xc_{Raman}/ % as predicted by the univariate chemometric model, were used for generating the multivariate calibration model. FT Raman spectra were vector normalized and the first derivatives of the spectra were calculated for all pre-calibrations. Not the total spectral range from 3500- 150 cm^{-1} was used to perform the PLS studies. We preferred to select the small spectral region 1510- 1210 cm^{-1} because of its strong crystallinity dependence, which turned out to improve the prediction of results. The accuracy of the

established calibration model it was validated by using a cross-validation method. The validation statistics described the resultant calibration model with good fits (R^2 = 0.9805) and with low error between modelled and reference values described by the **R**oot **M**ean **S**quare **E**rror of **C**ross **V**alidation, RMSECV = 2.04.

Table 1: Degree of crystallinity Xc/ % of different cellulose materials determined by ^{13}C NMR and FT Raman spectroscopy utilizing univariate and multivariate methods for the analysis of FT Raman spectral data.

Cellulose	Xc_{NMR} / %	Xc_{Raman} / % univariate	Xc_{Raman} / % multivariate
Elcema F100	26 %	23 %	28 %
Elcema F150	32 %	18 %	30 %
Vitacell A 300	29 %	21 %	30 %
Vivapur 102	60 %	59 %	55 %
Avicel PH 200	59 %	59 %	58 %
Avicel PH 301	62 %	52 %	57 %
Bacterial cellulose	72 %	69 %	69 %
Buckey Linters	60 %	56 %	58 %
Cotton Linters	67 %	50 %	61 %
Borregard	55 %	51 %	54 %

Determination of the Degree of Substitution (DS) of Cellulose Derivatives - Multivariate Calibration Models

FT Raman spectra of cellulose derivatives like carboxymethylcellulose (CMC) and cellulose acetate (CA) were also recorded. The degrees of substitution of CMC[20] and CA[21] were determined through NMR measurements. Multivariate chemometric models for the determination of DS_{CMC} and DS_{CA} were obtained by applying the PLS algorithm of the BRUKER software OPUS/Quant 2 to the FT Raman spectral data of the calibration samples. In both cases cross-validation was used for the verification of the predictions of the calibration model.[19]

In Figure 5 (left) an example of a FT Raman spectrum of a carboxymethylcellulose is presented. Typical Raman signals which characterise the pattern of substitution were observed at the frequency ranges of $\nu(COO^-)$, ν(C-O) and γ(C-C) modes. Consequently, the wave number range 1730- 800 cm^{-1} of the spectra was utilized for the development of the multivariate calibration model. A PLS regression algorithm was applied for finding the

best correlation function between the vector normalized FT Raman data and the corresponding DS values of the carboxymethylcellulose.

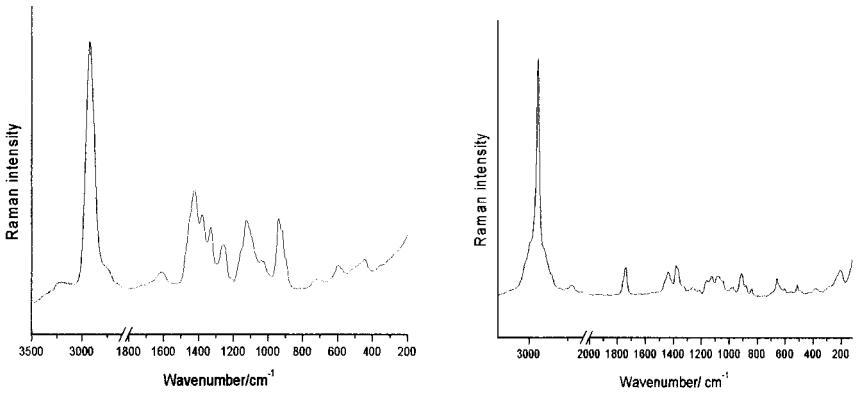

Figure 5. Exemplarily FT Raman spectra of a carboxymethylcellulose (left) and a cellulose acetate (right).

The calibration model was evaluated by cross–validation. As a result, a multivariate calibration model for predicting DS_{CMC} values in the range of 0.39 – 2.00 with high accuracy (R^2 = 0.9779) and low error between modelled and reference values (RMSECV = 0.0815) could be developed.

A similar calibration model for determining the degree of substitution of cellulose acetate DS_{CA} in the range of 1.25 – 2.90 was generated. For this purpose, the FT Raman spectral data were pre-calibrated by calculating their second derivatives. As depicted in Figure 5 (right), the frequency range of 1860- 1275 cm^{-1} of ν (C=O) is most suitable for the calibration procedure. The final cross-validation statistics certified a calibration model of high accuracy (R^2 = 0.959) and with low error between the modelled and reference values (RMSECV = 0.119) for the fast prediction of DS_{CA} values.

Prediction of Cellulose Reactivity

Cellulose reactivity is one of the most important properties of cellulose which strongly influence the industrial application processes. Therefore, it is important to develop analytical methods which are rapidly able to discriminate between cellulose materials of different reactivity level.

15 cellulose samples whose reactivity was determined by examining the change of molecular mass distribution within the mercerisation process were chosen for these experiments. The determination of reactivity as well as the process of mercerisation were discussed elsewhere.[22] An uniform decrease in the molecular weight was observed for one group of the cellulose samples after 15 and 30 minutes of mercerisation. These samples, found to be highly reactive because of their good accessibility to sodium hydroxide, see Figure 6 (left). The second group showed nearly no decrease in the molecular weight after 15 minutes, and only a small decrease after 30 minutes of mercerisation. These cellulose samples were described as being low in reactive, see Figure 6 (right).

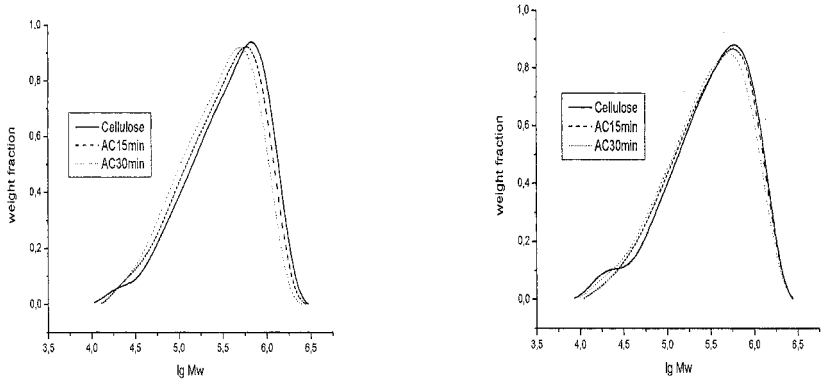

Figure 6. Molecular weight distribution of native cellulose after NaOH treatments of 15 and 30 minutes; highly reactive cellulose (left) and cellulose of low reactivity (right).

FT Raman vibrational spectra also pattern recognition techniques like clustering were tested in an effort to find methods capable of rapidly predicting cellulose properties. Using these techniques, samples can be classified according to a specific property by measurements indirectly related to the property of interest. An empirical relationship or classification rule can be developed from a set of samples for which the property of interest and the measurements are known. The classification rule can then be used to predict the property in samples that are not part of the original training set.[24]

A rapid prediction method for cellulose reactivity was developed using the BRUKER software package OPUS/ IDENT. A hierarchical cluster analysis usually is the most popular technique. Its basic objective is to discover sample groupings within the utilized data. Ward`s algorithm calculating the spectral distances between the clusters was applied to the FT Raman spectral data set of the 15 cellulose samples of different reactivity. The spectra were pre-treated by calculating their second derivatives. The training set for the prediction of cellulose reactivity was obtained using the frequency range 1550-1210cm^{-1} prominent for determining cellulose crystallinity.

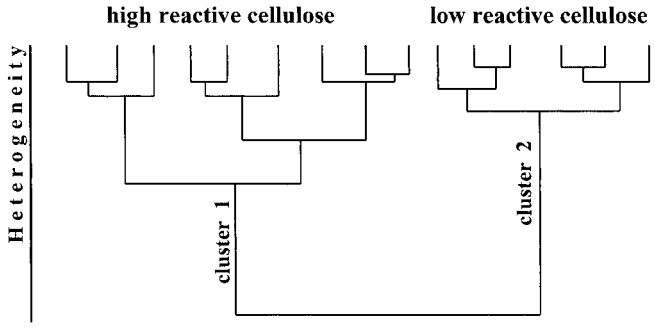

Figure 7. Dendrogram of the FT Raman spectral data set of 15 cellulose. The dendrogram was generated using BRUKER software OPUS/ IDENT and Ward`s algorithm.

The dendrogram of the training set is presented in Figure 7. Here, it is evident that the 15 cellulose samples are divided into two categories. Corresponding to the chemically determined reactivity their cluster membership derived from the FT Raman spectral data can be directly correlated to high or low reactivity of the cellulose material within the process of mercerisation. This training set was successfully tested by employing cellulose with chemically determined reactivity which were then subjected to the cluster analysis and were ranged to its category for validation.[25]

Investigations of Cellulosic Plant Fibres

In Europe, the main annual bast fibre crops are flax (*Linum usitatissimum* L.) and hemp (*Cannabis sativa* L.). Apart from traditional textile applications, the fibres of these plants are increasingly used in different technical products. Today, they are recognized as a potential replacement for glass fibres e.g. for use as reinforcing component of composite

materials. The fibres have certain advantages over glass fibres such as low cost, high tensile strength-to-weight ratio, biodegradability and easy use for processing. However, practical applications of flax and hemp are still limited by the natural inhomogeneities of the plant material. Specific analytical methods are necessary for determining the fibre properties, for controlling fibre qualities and the resulting technical products.

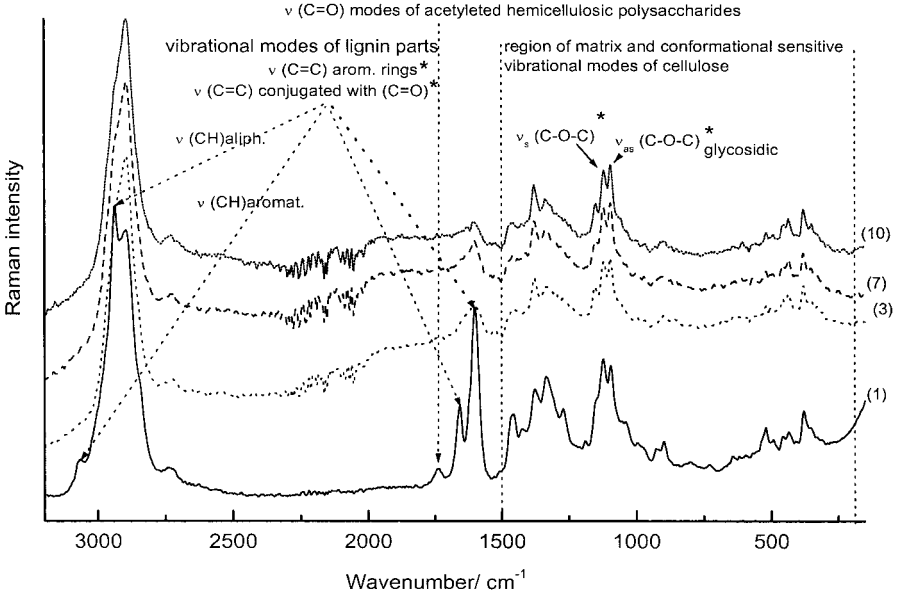

Figure 8. FT Raman spectra of non-retted flax fibres mechanically treated for (1), (3), (7) and (10) times. Important frequency ranges and characteristic Raman lines are denoted.

Previous FT Raman spectroscopic investigations have demonstrated the feasibility of the method for monitoring molecular structures of the tissues of flax stems *in situ* and for following molecular changes of cellulosic fine structure of the fibres caused by aging and mechanical as well as chemical processing. [11, 14, 26, 27]

The FT Raman spectrum of the fibres has to be considered as a superposition of the vibrational spectra of all cell wall components of the bast fibres. Thus, the vibrational modes of cellulosic, hemicellulosic and pectic carbohydrates along with those of residual parts of lignin are observed, as it is presented in Figure 8.

Relative intensity measurements were carried out on normalized fibre spectra in order to

determine differences of the molecular fibre composition. Various intensity ratios were calculated using vibrational modes of β(1→4) glycosidic linkages $\nu_{s;as}$(COC), CH stretching vibrations of cellulose ν(CH) as well as the aromatic ring stretching mode of lignin components ν (C=C) by means of curve fitting. As represented in previous works,

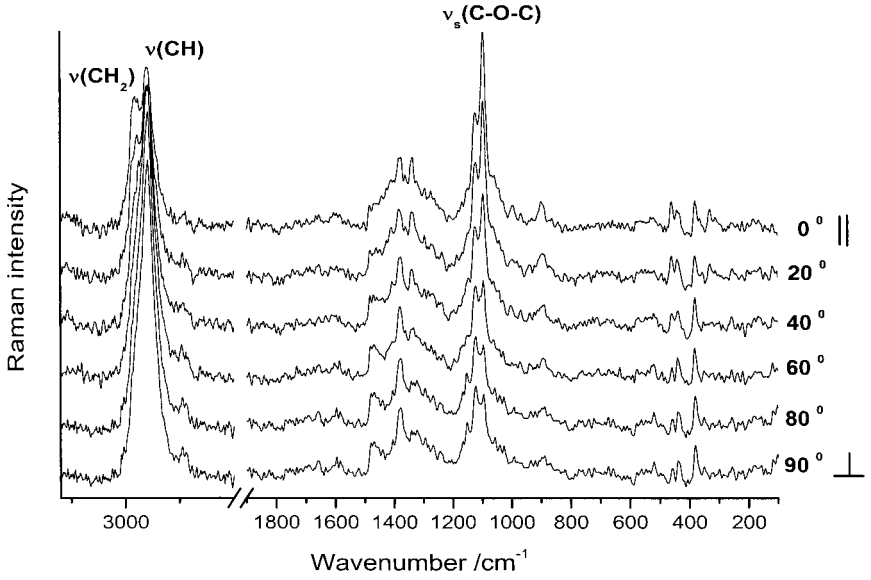

Figure 9. Orientation dependent micro FT Raman spectra of a single hemp fibre. Spectra of the parallel oriented fibre were recorded under different polarisation angles of the exciting laser beam.

Raman intensity ratios $R_1 = I^{\nu as(COC)}/I^{\nu s(COC)}$, $R_2 = I^{\nu(C=C)}/I^{\nu s(COC)}$ and $R_3 = I^{\nu s(COC)}/I^{\nu(CH)}$ may be used as spectral parameters characterizing changes of molecular composition of the fibre surfaces as well as changes in degree of molecular order within the cellulosic structures of the fibres dependent on the application of alkaline treatments and fibre refining agents as well as on the degree of fibre maturity. [11, 14, 28, 29]

Furthermore, micro FT Raman intensity ratios of single fibre filaments may be used. As shown in Figure 9, the intensity of several Raman lines is strongly dependent on the orientation of the E-vector of the exciting beam relative to the fibre axis. From these measurements, the orientation of the corresponding atomic groups of the cellulose

skeletons with respect to the fibre axes can be determined. Observing the orientation dependent vibrational behaviour of ν_s(C-O-C), ν(CH) and $\nu_s(CH_2)$ modes, mainly related to $\beta(1\rightarrow4)$ glycosidic linkages of the cellulose skeletons, to methine groups of the glucopyranose rings as well as to the methylene groups of the glucopyranose side chains, it can be shown that the glycosidic linkages of the cellulose skeletons are nearly parallel oriented with respect to the fibre axes. A parallel orientation was found for the methylene groups of the glucopyranose side chains, which is not the case for the methine groups of the glucopyranose units. They are mainly perpendicularly oriented to the fibre axes as indicated by the strongest intensity of the ν(CH) mode if the E-vector of the exciding beam is also perpendicularly oriented.

Raman spectroscopy has been successfully used for the analysis of deformation processes in a variety of high-performance polymer fibres as well as in plant fibres. It has been reported that Raman lines associated with the backbone groups of polymer molecules shift in wave number due to the application of stress or strain.[30, 31]

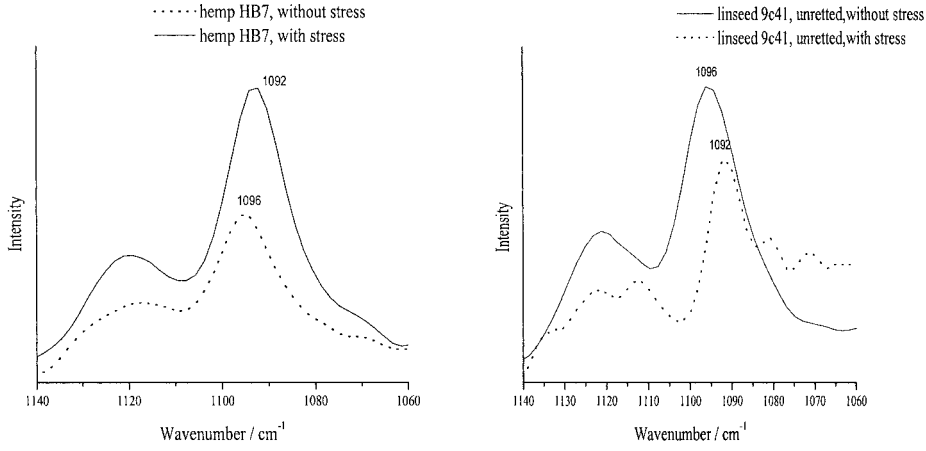

Figure 10. Micro FT Raman spectra of single hemp fibres (left) and single linseed fibres (right) measured with and without strain. Typical Raman shifts due to stress development are indicated.

This behaviour can be interpreted as being the result of macroscopic deformation of the polymer fibre causing chain stretching and /or crystal rotation in the polymer molecules in

the fibre. Hence it can be used as method for relating macroscopic and molecular deformation processes. [32]

The Raman frequency shift of ν (C-O-C) stretching modes of single hemp and linseed fibres due to the increasing stress are presented in Figure 10. A straining rig was used under the FT Raman microscope for the stress experiments. The results of the experiments indicate that the macroscopic deformation of hemp and linseed fibres is translated directly into molecular deformation of the cellulose skeletons.

Thus, vibrational modes which characterize C-O-C stretching motions of the glucopyranose rings as well as of the glycosidic linkages are clearly involved, and may be used for the calibration of internal micro-strains or stresses. Our FT Raman experiments confirmed related results using micro Raman spectroscopy with visible laser excitation.[31]

Conclusions

The results reported in this work clearly demonstrate that FT Raman spectroscopy / micro spectroscopy are effective methods for the characterization of native cellulose, pulps, cellulose derivatives and cellulosic plant material.

The important advantages of FT Raman spectroscopy are the ease of sample preparation and the short time required for the measurements. The effective combination of macroscopic and microscopic tools as well as the possibility for on line process control will establish this analytical method for production and quality control of all processes in which changes of conformational arrangements and molecular compositions of cellulose occur.

For the first time univariate and multivariate calibration models were developed utilizing FT Raman spectral data for determining the degree of cellulose I crystallinty Xc_{Raman} and the degrees of substitution $DS_{CMC;\,CA}$ for native cellulose and cellulose derivatives.

Orientation dependent micro Raman experiments on cellulose fibres may be used for the detailed information about the arrangements of molecular groups at the fibre surfaces.

Micro Raman measurement of stress induced Raman shifts of cellulosic plant fibres may be used for the determination of micromechanical properties of the plant material.

[1] J. Blackwell, P. D. Vasko, J. L. Koenig, *J. Appl. Phys.* **1970**, 41, 4375.
[2] R. H. Atalla, *App. Polym. Symp.* **1976**, 28, 659.
[3] R. H. Atalla, *J. Appl. Polym. Sci., Appl. Polym. Symp.* **1983**, 37, 295.
[4] R. H. Atalla, J. Ranua, E.W. Malcolm, *Tappi J.* **1984**, 67, 96.
[5] J. H. Wiley, R.H. Atalla, *Carbohydr. Res.* **1987**, 160, 113.

[6] J. H. Wiley, R.H. Atalla, *ACS Symp. Ser.* **1987**, 340, 151.
[7] R. H. Atalla, in: „Cellulose", J. F. Kennedy, G.O. Phillips, P.A. Williams, Eds., Ellis Horwood, Chichester 1989, 61 pp.
[8] U.P. Agarwal , R.H. Atalla, *Planta* **1986**, 169, 325.
[9] R.H. Atalla, R.E. Whitmore, C.J. Heimbach, *Macromolecules* **1980**, 13, 1717.
[10] B. Schrader, in: „Infrared and Raman Spectroscopy - Methods and Applications", B. Schrader, Ed. VCH Weinheim, New York, Basel, Cambridge, Tokyo, 1995, p. III/ 155 pp.
[11] H.G.M. Edwards, D.W. Farwell, D. Webster, *Spectrochim. Acta* **1997**, 53A , 2383.
[12] E. Urlaub, J. Popp, W. Kiefer, G. Bringmann, D. Koppler, H. Schneider, U. Zimmermann, B. Schrader, *Biospectroscopy* **1998**, 4, 113.
[13] K. Schenzel, S. Fischer, *Cellulose* **2001**, 8, 49.
[14] A. Jähn, M Füting, K.Schenzel, W. Diepenbrock, *Spectrochim. Acta* **2002**, 58A, 2271.
[15] S. Fischer, W. Voigt, K. Fischer, *Cellulose*, **1999**, 1, 3.
[16] S. Fischer, H. Leipner, K. Thümmler, E. Brendler, J. Peters, *Cellulose*, **2003**, 10, 227.
[17] S. Fischer, H. Leipner, E. Brendler, W. Voigt, K. Fischer , *ACS Symp. Ser.* **1999**, 10, 737.
[18] K. Schenzel, S. Fischer, E. Brendler, *Cellulose* **2005,** in print.
[19] K. Schenzel, S. Fischer, K. Fischer, CSIRO Publishing, *XIXth International Conference on Raman Spectroscopy*, **2004**, Australia, Proceedings p. 415.
[20] A. Baar, W.-M. Kulicke, K. Szablikowski, R. Kiesewetter, *Macromol. Chem. Phys.* **1994,** 195, 1483.
[21] J.Kunze, A. Ebert, H.-P. Fink, *Cell. Chem.Technol.* **2000**, 34, 21.
[22] K.Fischer, H. Hinze, I. Schmidt, *Das Papier* **1994**, 48, 769.
[23] S.Fischer, H.Leipner, E. Brendler, W. Voigt, K. Fischer, S.Spange, K.Schenzel, *Das Papier* **2001**, 4, 61.
[24] B.K. Lavine, in: „Encyclopedia of Analytical Chemistry", R. A. Meyer, Ed., J. Wiley & Sons **2000,** Chichester.
[25] K. Schenzel, S. Fischer, *223rd ACS National Meeting* **2002** *Orlando,* Abstracts of Papers, CELL-074.
[26] D.S. Himmelsbach, D.E. Akin, J. *Agric. Food Chem.* **1998**, 46, 991.
[27] B. Schrader, H. H. Klump, K. Schenzel, H. Schulz, *J. Mol. Struct.* **1999**, 501, 201.
[28] K.S.Kumar, K.Schenzel, E.Grimm, W.Diepenbrock CSIRO Publishing, *XIXth International Conference on Raman Spectroscopy*, **2004**, Australia, Proceedings p. 417.
[29] A. Jähn, K. Schenzel, W. Diepenbrock, *9th European Conference on Spectroscopy of Biological Molecules*, **2002** Prag, Book of Abstracts p. B 269.
[30] R. J. Young, in: "*Polymer Surfaces and Interfaces II*", W.J. Feast, H.S. Munro, R. W. Richards, Eds. J. Wiley & Sons, Chichester, New York 1993, p. 6/ 131 pp.
[31] S. J. Eichhorn, M. Hughes, R. Snell, L. Mott, *J. Mat. Sci. Lett.* **2000**, 19, 721.
[32] W. Y. Hamad, *Int. Conferenece on Composite Materials*, **1997,** Australia, Proceedings p. IV-598.